Porous Organic Cage Compounds

DOI: 10.1002/anie.201308924

A Permanent Mesoporous Organic Cage with an Exceptionally High Surface Area**

*Gang Zhang, Oliver Presly, Fraser White, Iris M. Oppel, and Michael Mastalerz**

Abstract: *Recently, porous organic cage crystals have become a real alternative to extended framework materials with high specific surface areas in the desolvated state. Although major progress in this area has been made, the resulting porous compounds are restricted to the microporous regime, owing to the relatively small molecular sizes of the cages, or the collapse of larger structures upon desolvation. Herein, we present the synthesis of a shape-persistent cage compound by the reversible formation of 24 boronic ester units of 12 triptycene tetraol molecules and 8 triboronic acid molecules. The cage compound bears a cavity of a minimum inner diameter of 2.6 nm and a maximum inner diameter of 3.1 nm, as determined by single-crystal X-ray analysis. The porous molecular crystals could be activated for gas sorption by removing enclathrated solvent molecules, resulting in a mesoporous material with a very high specific surface area of 3758 $m^2 g^{-1}$ and a pore diameter of 2.3 nm, as measured by nitrogen gas sorption.*

The self-assembly of smaller molecular subunits into larger supramolecular entities with the shape of Platonic or Archimedian bodies has been the focus of several studies in recent years, especially when the coordination of metal ions has been used for binding motifs.[1] By using the metal coordination motif, it was even possible to synthesize near-spherical coordination cage compounds with outer diameters of approximately five nanometers from rather simple molecular building blocks and metal cations.[2] In comparison to coordination cages, purely organic cages are much rarer, probably due to the fact that most covalent bonds are formed by irreversible reactions that do not allow a structural "self-correction", often accompanied by low overall yields in the cyclization step. Recently, the use of reversible formations of covalent bonds has been applied to synthesize organic cage compounds from small and readily accessible precursors in reasonable to very high yields.[3]

It has been demonstrated that some of those organic cage compounds are highly porous in the crystalline or amorphous state, when desolvated in vacuum,[4] with reported Brunauer–Emmett–Teller (BET) surface areas (SAs) of up to 2071 $m^2 g^{-1}$.[5] The solubility of porous organic molecules offers some advantages in comparison to insoluble network materials:[6] porous molecules are miscible in solution enabling adjustment of the properties of the material;[7] an exhaustive post-functionalization by chemical reactions in the inner cavities of the cage molecules allows the functional groups on the surface, and hence the gas sorption properties of the porous materials, to be changed.[8] Furthermore, processing of porous molecules into functional devices such as quartz crystal microbalances for the sensing of volatile analytes has been reported,[9] as has embedding them into membranes.[10]

When aiming for organic cages with very large pores, especially in the mesopore regime (> 2 nm), the prevention of a structural collapse of the molecules upon desolvation is one of the major obstacles one has to face.[11] There are very few reports on organic cages with cavity diameters > 2 nm, and none of these was reported as being permanently porous.[12] For example, Warmuth and co-workers synthesized organic cage compounds with solvodynamic diameters of approximately 4 nm, according to the diffusion coefficients measured by DOSY-NMR spectroscopy.[12a] However, the resulting cage compounds were not investigated in terms of porosity and no additional structural proof by single-crystal X-ray analysis could be provided. Cages of larger sizes, which were characterized in the solid state by X-ray diffraction of single-crystals were synthesized by the Cooper group,[12b] the Severin group,[12c] and Gawronski et al.[12d] (see also the Supporting Information, Figure S27). Whereas the Cooper cage had an outer diameter of 2.9 nm and inner diameter of 1.5 nm, which is similar to a previously reported [4+6] cage compound,[4c] the Gawronski cage was larger, especially when the inner cavity dimensions were taken into account (outer diameter: 3.0 nm, inner diameter: 1.7 nm). By a combination of metallasupramolecular chemistry and dynamic imine bond formation, Severin and co-workers prepared a cage with outer and inner diameters of 2.7 nm and 1.9 nm, respectively. Unfortunately, these larger cages failed to remain porous upon desolvation of the crystals: mainly nonporous compounds were observed, as has been verified by gas sorption measurements.

---

[*] Dr. G. Zhang, Prof. Dr. M. Mastalerz
Organisch-Chemisches Institut, Ruprecht-Karls-Universität
Heidelberg, Im Neuenheimer Feld 270
69120 Heidelberg (Germany)
E-mail: michael.mastalerz@oci.uni-heidelberg.de

Dr. O. Presly, Dr. F. White
Agilent Technologies, Yarnton (UK)

Prof. Dr. I. M. Oppel
Anorganische Chemie, RWTH Aachen
Landoltweg 1, 52056 Aachen (Germany)

[**] We would like to thank the German Research Council (Deutsche Forschungsgemeinschaft, DFG) and the "Fond der Chemischen Industrie" (FCI) for generous financial support. G.Z. would like to thank the Alexander-von-Humboldt foundation for a postdoctoral fellowship. Conny Egger and Samuel Blessing (both Ulm University) are acknowledged for performing nitrogen sorption measurements and collecting PXRD data. We are grateful to Benjamin Eberle (Heidelberg University) for TGA measurements.

Supporting information for this article is available on the WWW under http://dx.doi.org/10.1002/anie.201308924.

Herein, we demonstrate that an organic cage compound with an average inner pore diameter of 2.8 nm can be synthesized in one step from 20 rigid precursor molecules. The shape-persistent voids of the cage molecules stay intact upon desolvation, resulting in a permanent porous material with an extraordinarily high BET SA of 3758 $m^2 g^{-1}$ and a measured pore diameter of 2.3 nm, according to the Dubinin–Radushkevich equation, which is defined by IUPAC as mesoporosity.[13]

We started our investigation with tetraol precursor **1a** (for the synthesis, see Scheme S1) as a molecular building block. This is expected to give cuboctahedral cage compound **3a**, with cavities of a minimum inner diameter >2 nm owing to the molecular geometry in condensation with triboronic acid **2** (Figure 1 a). However, all condensation attempts (changing solvent, concentration, and reaction temperature) with the triboronic acid **2** gave no distinct signals in the ^{1}H NMR spectrum of the crude product. This assumes that intermediates of the desired cage compound are already insoluble, leading to no further reaction. We found that adding two additional ethyl chains in the 13- and 16-positions of the triptycene precursor (**1b**) is sufficient to drive the reaction to completion, resulting in full conversion of the precursors into the corresponding cage **3b** by a 48-fold condensation of twelve triptycene molecules **1b** and eight molecules of the triboronic acid **2**. The synthesis was performed by dispersing the insoluble reactants in chloroform and heating the resulting suspension to reflux until the reaction mixture became a clear solution. The solution was concentrated by evaporation of solvent on a rotary evaporator and precipitated with *n*-hexane. The white precipitate was collected on a Büchner funnel to give the product in quantitative yield. However, once the compound had precipitated it was difficult to redissolve. The characteristic peaks in the IR-spectrum of **3b** indicated the presence of catechol boronic ester units (see the Supporting Information). Furthermore, the measured elemental analysis was in good agreement to the calculated one (see the Supporting Information).

To characterize the compound in solution, we added deuterated tetrachloroethane to the chloroform solution and removed the chloroform on a rotary evaporator. The ^{1}H NMR spectrum of cage compounds **3b** is relatively simple, and showed only three peaks in the aromatic region ($\delta = 8.83$ ppm, 7.42 ppm and 6.82 ppm) and one signal that can be clearly assigned to the bridgehead protons of the triptycene units ($\delta = 5.72$ ppm; Figure 2 a). By the addition of an internal standard (mesitylene) we calculated that the cage

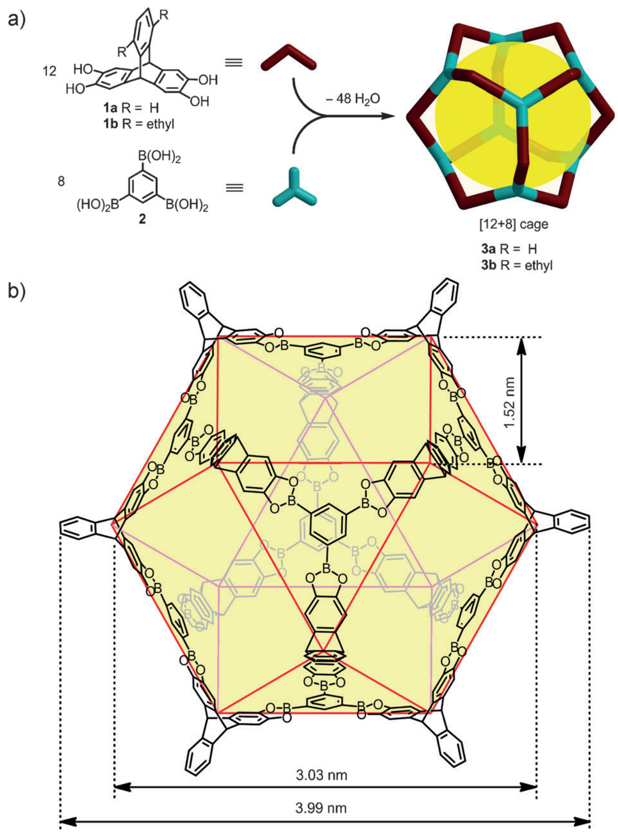

Figure 1. a) One-step 48-fold condensation reaction of twelve molecules of triptycene tetraol **1a** or **1b** with eight molecules of the triboronic acid **2** to the cuboctahedral [12+8] cages **3a** and **3b**, respectively. b) The scaffold of the cuboctahedral cage with selected dimensions: outer diameter (3.99 nm), inner maximum diameter (3.03 nm), and open quadric windows of 1.52 nm. Edges of the cuboctahedral geometry are highlighted in red. The shown dimensions are based on an AM1-optimized model (see the Supporting Information).

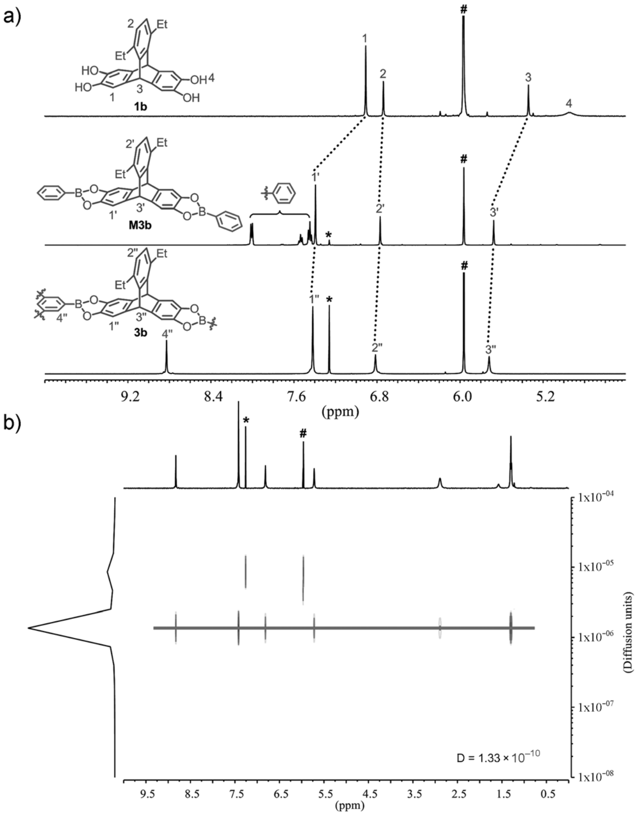

Figure 2. a) Comparison of the aromatic and bridgehead regions of the ^{1}H NMR spectra of reactant **1b** (heterogeneous), model compound **M3b**, and cage compound **3b** in $C_2D_2Cl_4$. For full spectra, see the Supporting Information. b) DOSY NMR spectrum of cage compound **3b** in $C_2D_2Cl_4$. The hash (#) symbols mark residual non-deuterated tetrachloroethane. The asterisks mark residual chloroform.

compound had formed in 94% in solution. Comparing the NMR spectrum with that of the model compound **M3b**, we assumed that all diol units had been turned into the corresponding catechol boronic ester units, which is also suggested by the integrals of the peaks. In principle, from the ^{1}H NMR spectrum we can only conclude that the correct ratio (2:3) of molecular reactants is found in the product formed, which could be any $[3n(\mathbf{1b}) + 2n(\mathbf{2})]$ condensation product. Unfortunately, no mass spectrum could be recorded showing the molecular peak, which may be due to the fact that the molecule bears 24 catechol boronic ester units, each of which is relatively easily chemically cleaved. Therefore, we recorded a DOSY NMR spectrum of compound **3b** to get more structural information for the molecule (Figure 2b). The spectrum showed only one trace of signals with a diffusion coefficient of $D = 1.33 \times 10^{-6}$ cm^2 s^{-1}, corresponding to a solvodynamic radius of 1.27 nm, which is in good agreement with the minimum inner diameter of 2.6 nm of the sphere of a [12+8] cage compound as depicted in Figure 1a.[14]

The structure of cage compound **3b** was also determined by single-crystal X-ray diffraction. Single-crystals of **3b** were grown by vapor diffusion of *n*-hexane into a saturated solution of **3b** in chloroform. Owing to the porous nature of this material, the crystals contain large amounts (72% of the unit cell) of disordered solvent, and therefore the structure was treated using the SQUEEZE function of PLATON to remove the electron density of the solvate molecules.[15] Additionally, it was necessary to use constraints to control the geometry of aromatic rings and restraints to enforce chemically sensible bond lengths and angles in the ethyl chains in particular. Vibrational restraints were also used to control atomic displacement parameters across the molecule, which was high, presumably due to the large and spherical nature of the molecule allowing considerable motion. The compound crystallizes in the triclinic space group *P-1* with one molecule in the unit cell.[16] The cavity of the molecule is very large in comparison with other porous cage compounds, with an inner diameter of 2.4–2.6 nm between two opposite aryl rings of the triboronic ester units and 2.9–3.1 nm between the bridgehead atoms of two opposite triptycene units (Figure 3). The pore window to the cavity is approximately 1.7 nm in diameter. The molecules pack through π–π interactions along the crystallographic *c* axis, which is reflected in a staggered coplanar assembling of boronic ester units of adjacent molecules at a distance of 3.2–3.4 Å. Along other axes, the packing interactions are rather weak, which can mainly be assigned as CH–π interactions. For π–π interactions, 3.2 Å is relatively short, thus revealing that this interaction is relatively strong in comparison to existing CH–π interactions.

As mentioned above, shape-persistency during evacuation for molecules of such dimensions has not been reported thus far. Because of the geometrical shape of an Archimedian body, we expected that it should be possible for it to remain as a stable porous material after removing enclathrated solvent molecules from **3b**. To prevent the crystalline material from thermal stress, we activated it by immersing (12 h × 6) in *n*-pentane before evacuating at room temperature, then measuring the nitrogen sorption of the material; as has been previously described for a hydrogen-bonded network with very high specific surface area.[17] The measured isotherm (Figure 4) can best be described as a type I isotherm.[13] The

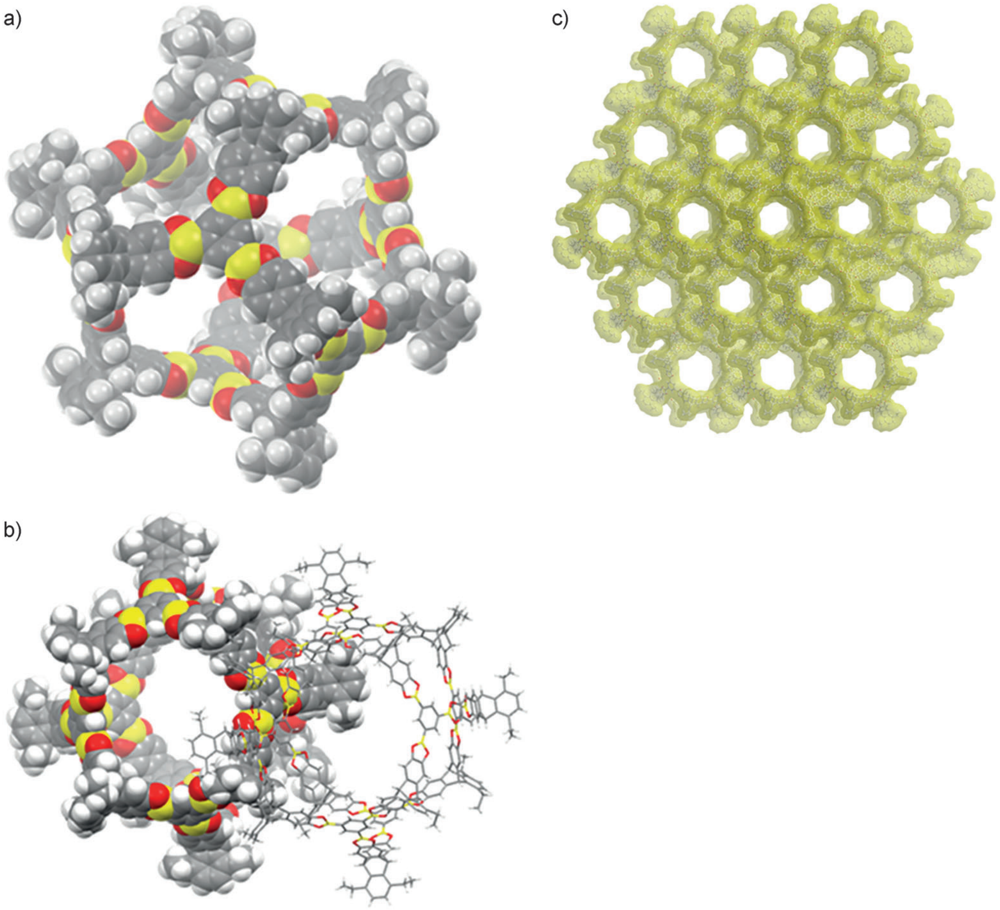

Figure 3. Single-crystal X-ray structure of solvated cage **3b**. Enclathrated solvent molecules were disordered and could not be refined. a) Space-filling model. C gray, H white, O red, B yellow. b) Molecular packing of cage **3b** in solid state. One cage is depicted as a stick representation. c) Packing in the solid state. The yellow surface represents a solvent-accessible surface with a probe radius of 1.8 Å.

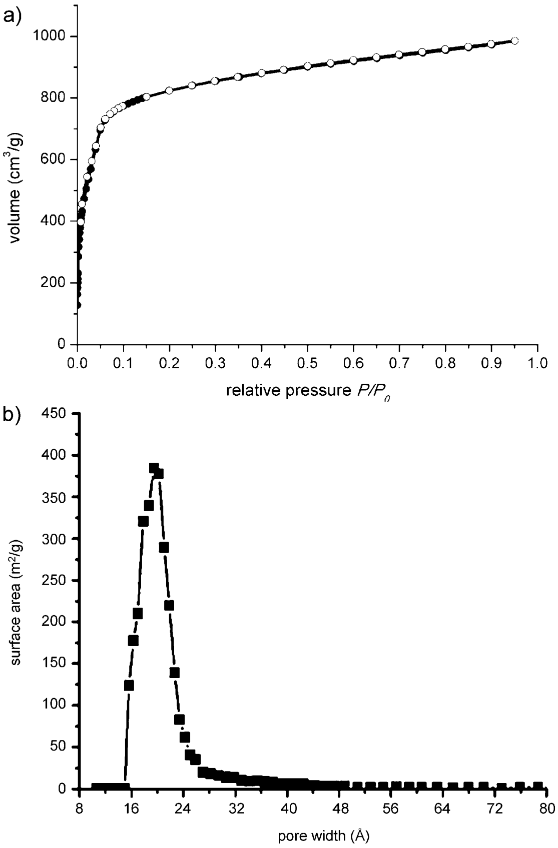

Figure 4. a) Nitrogen gas sorption isotherm at 77 K for cage **3b**. Closed symbols represent adsorption, open symbols represent desorption. b) The NLDFT pore-size distribution.

specific surface area is 3758 m^2g^{-1}, when the BET model is considered, and 4246 m^2g^{-1} using the Langmuir model. The pore volume is $V_{pore} = 1.41$ cm^3g^{-1}, which is comparable to that determined from the X-ray single-crystal structure by applying the program crystal explorer (1.57 cm^3g^{-1}).[18] NLDFT calculations (N_2 adsorption branch at 77 K, spherical pores, silica material) gave a maximum pore diameter of 2.03 nm with a low fitting error (1.27%). It seemed more reasonable to us to determine the pore size by using the Dubinin–Radushkevich (DR) equation,[19] which is a highly-applicable method for porous materials with homogeneous pore structures, as it is the case for crystalline **3b**. Using this method, the average pore diameter of the material was determined to be 2.3 nm, which is in good agreement with the molecular pore size determined from the X-ray crystal structure of solvate **3b**. The crystalline phases of the desolvated and solvated structures are not the same, as has been found by powder X-ray diffraction (PXRD). However, owing to the accordance of the measured pore size, both by NLDFT and DR methods to that calculated from the solvated phase, it is suggested that the molecular cages retain their shape and remain intact during evacuation, but the assembling of the cages in the desolvated phase have changed. Solving crystal structures from PXRD data of such structures is not trivial, and further work will be done to get more insight into the occurring phase change during evacuation. The shape of the sorption isotherms is similar to that reported for MIL-101, and the pore dimensions and surface areas of the cage compound **3b** are indeed comparable to MIL-101 (V_{pore} = 2.0 cm^3g^{-1}; BET SA = 4100 m^2g^{-1}).[20] All data are readily reproducible, as has been demonstrated by the synthesis and measurement of a second batch sample (BET SA = 3475 m^2g^{-1}). The specific surface area of **3b** is higher than for COF-102 (BET SA = 3472 m^2g^{-1}),[21] and is the highest reported thus far for any porous cage compound. To the best of our knowledge, **3b** also represents the first single-crystal X-ray structure of any reported crystalline porous organic material based on the formation of boronic esters.

In conclusion, we have shown that it is possible to synthesize a shape-persistent, discrete mesoporous organic cage compound by dynamic covalent formation of 24 boronic ester units in one step. The resulting BET specific surface area of 3758 m^2g^{-1} is the highest reported thus far for any porous organic molecules. Currently, we are working on the synthesis of even larger porous cages to gain further insight into the scope and limitations of this new and fascinating class of porous materials.

Received: October 13, 2013

Keywords: boronic acids · cage compounds · dynamic covalent chemistry · porosity · triptycene

---

[1] For recent reviews on supramolecular coordination cages, see: a) R. Chakrabarty, P. S. Mukherjee, P. J. Stang, *Chem. Rev.* **2011**, *111*, 6810–6918; b) M. M. J. Smulders, I. A. Riddell, C. Browne, J. R. Nitschke, *Chem. Soc. Rev.* **2013**, *42*, 1728–1754; c) R. W. Saalfrank, H. Maid, A. Scheurer, *Angew. Chem.* **2008**, *120*, 8924–8956; *Angew. Chem. Int. Ed.* **2008**, *47*, 8794–8824.

[2] a) B. Olenyuk, M. D. Levin, J. A. Whiteford, J. E. Shield, P. J. Stang, *J. Am. Chem. Soc.* **1999**, *121*, 10434–10435; b) Q.-F. Sun, J. Iwasa,, D. Ogawa, Y. Ishido, S. Sato, T. Ozeki, Y. Sei, K. Yamaguchi, M. Fujita, *Science* **2010**, *328*, 1144–1147; c) S. Pasquale, S. Sattin, E. C. Escudero-Adán, M. Martinez-Belmonte, J. de Mendoza, *Nat. Commun.* **2012**, *3*, 785, DOI: 10.1038/ncomms1793.

[3] For reviews on organic cage compounds, see: a) M. Mastalerz, *Angew. Chem.* **2010**, *122*, 5164–5175; *Angew. Chem. Int. Ed.* **2010**, *49*, 5042–5053; b) N. M. Rue, J. Sun, R. Warmuth, *Isr. J. Chem.* **2011**, *51*, 743–768; for selected recent examples, see: c) K. Acharyya, S. Mukherjee, P. S. Mukherjee, *J. Am. Chem. Soc.* **2013**, *135*, 554–557; d) Y. Jin, B. A. Voss, R. D. Noble, W. Zhang, *Angew. Chem.* **2010**, *122*, 6492–6495; *Angew. Chem. Int. Ed.* **2010**, *49*, 6348–6351; e) Y. Jin, B. A. Voss, A. Jin, H. Long, R. D. Noble, W. Zhang, *J. Am. Chem. Soc.* **2011**, *133*, 6650–6658; f) Y. Jin, A. Jin, R. M. McCaffrey, H. Long, W. Zhang, *J. Org. Chem.* **2012**, *77*, 7392–7400; g) Z. Lin, J. Sun, B. Efremovska, R. Warmuth, *Chem. Eur. J.* **2012**, *18*, 12864–12872; h) A. Granzhan, C. Schouwey, T. Riis-Johanessen, R. Scopelliti, K. Severin, *J. Am. Chem. Soc.* **2011**, *133*, 7106–7115.

[4] For examples of porous cage compounds with very high specific surface areas (> 600 m^2g^{-1}), see: a) T. Tozawa, J. T. A. Jones, S. I. Swamy, S. Jiang, D. J. Adams, S. Shakespeare, R. Clowes, D. Bradshaw, T. Hasell, S. Y. Chong, C. Tang, S. Thompson, J. Parker, A. Trewin, J. Bacsa, A. M. Z. Slawin, A. Steiner, A. I. Cooper, *Nat. Mater.* **2009**, *8*, 973–979; b) M. W. Schneider, I. M. Oppel, M. Mastalerz, *Chem. Eur. J.* **2012**, *18*, 4156–4160; c) M.

Mastalerz, M. W. Schneider, I. M. Oppel, O. Presly, *Angew. Chem.* **2011**, *123*, 1078–1083; *Angew. Chem. Int. Ed.* **2011**, *50*, 1046–1051; d) M. J. Boyds, M. E. Briggs, J. T. A. Jones, D. J. Adams, S. Y. Chong, M. Schmidtmann, A. I. Cooper, *J. Am. Chem. Soc.* **2011**, *133*, 16566–16571; e) J. T. A. Jones, T. Hasell, X. Wu, J. Bacsa, K. E. Jelfs, M. Schmidtmann, S. Y. Chong, D. J. Adams, A. Trewin, F. Schiffman, F. Cora, B. Slater, A. Steiner, G. M. Day, A. I. Cooper, *Nature* **2011**, *474*, 367; f) M. W. Schneider, H.-J. S. Hauswald, R. Stoll, M. Mastalerz, *Chem. Commun.* **2012**, *48*, 9861–9863; g) A. Avellaneda, P. Valente, A. Burgun, J. D. Evans, A. W. Markwell-Heys, D. Rankine, D. J. Nielsen, M. R. Hill, C. J. Sumby, C. J. Doonan, *Angew. Chem.* **2013**, *125*, 3834–3837; *Angew. Chem. Int. Ed.* **2013**, *52*, 3746–3749.

[5] M. W. Schneider, I. M. Oppel, H. Ott, L. G. Lechner, H.-J. S. Hauswald, R. Stoll, M. Mastalerz, *Chem. Eur. J.* **2012**, *18*, 836–847.

[6] J. R. Holst, A. Trewin, A. I. Cooper, *Nat. Chem.* **2010**, *2*, 915–920.

[7] T. Hasell, S. Y. Chong, K. E. Jelfs, D. J. Adams, A. I. Cooper, *J. Am. Chem. Soc.* **2012**, *134*, 588–598.

[8] M. W. Schneider, I. M. Oppel, A. Griffin, M. Mastalerz, *Angew. Chem.* **2013**, *125*, 3699–3703; *Angew. Chem. Int. Ed.* **2013**, *52*, 3611–3615.

[9] M. Brutschy, M. W. Schneider, M. Mastalerz, S. R. Waldvogel, *Adv. Mater.* **2012**, *24*, 6049–6052.

[10] A. F. Bushell, P. M. Budd, M. P. Attfield, J. T. A. Jones, T. Hasell, A. I. Cooper, P. Bernardo, F. Bazzarelli, G. Clarizia, J. C. Jansen, *Angew. Chem.* **2013**, *125*, 1291–1294; *Angew. Chem. Int. Ed.* **2013**, *52*, 1253–1256.

[11] M. Mastalerz, *Chem. Eur. J.* **2012**, *18*, 10082–10091.

[12] a) Y. Liu, X. Liu, R. Warmuth, *Chem. Eur. J.* **2007**, *13*, 8953–8959; b) K. E. Jelfs, X. Wu, M. Schmidtmann, J. T. A. Jones, J. E. Warren, D. J. Adams, A. I. Cooper, *Angew. Chem.* **2011**, *123*, 10841–10844; *Angew. Chem. Int. Ed.* **2011**, *50*, 10653–10656; c) A. Granzhan, T, Riis-Johannessen, R. Scopelliti, K. Severin, *Angew. Chem.* **2010**, *122*, 5647–5650; *Angew. Chem. Int. Ed.* **2010**, *49*, 5515–5518; d) P. Skowronek, B. Warżajtis, U. Rychlewska, J. Gawroński, *Chem. Commun.* **2013**, *49*, 2524–2526.

[13] K. S. W. Sing, D. H. Everett, R. A. W. Haul, L. Moscou, R. A. Pierotti, J. Rouquerol, T. Simieniewska, *Pure Appl. Chem.* **1985**, *57*, 603–619.

[14] A. Macchioni, G. Ciancaleoni, C. Zuccaccia, D. Zuccaccia, *Chem. Soc. Rev.* **2008**, *37*, 479–489.

[15] a) P. Van der Sluis, A. L. Spek, *Acta Crystallogr. Sect. A* **1990**, *46*, 194–201; b) A. L. Spek, *Acta Crystallogr. Sect. D* **2009**, *65*, 148–155.

[16] Agilent Technologies, (2013), CrysAlisPro Software system, version 1.171.36.28, Agilent Technologies UK Ltd, Oxford, UK. Crystal structure of **3b**: dark red prisms, 0.218 × 0.147 × 0.042 mm^3, triclinic, $P\bar{1}$, $a=27.7864(11)$, $b=27.8540(17)$, $c=29.3623(19)$ Å, $\alpha=111.469(6)$, $\beta=101.316(4)$, $\gamma=105.397(4)$°, $V=19268.5(19)$ Å3, $Z=1$, $\rho_{calc}=0.457$ g cm^{-}3, $\theta_{max}=36.37$°, λ-(Cu$_{K\alpha}$) = 1.5418 Å, $T=90(2)$ K, 30055 measured reflections, 18309 independent reflections ($R_{int}=0.0279$), 8600 reflections $[I>2\sigma(I)]$, 549 parameter, $R=0.1250$, wR = 0.3461 (for all data). Data were collected on an Agilent Technologies SuperNova A diffractometer using Cu radiation with an Oxford Cryosystems Cryostream low-temperature device operating at 100 K. Data were processed using the CrysAlisPro software package, solved with SUPERFLIP and refined using SHELX and the OLEX2 refinement programs. X-ray data have been deposited at the Cambridge Crystallographic Data Centre (CCDC 948612 contains the supplementary crystallographic data for this paper. These data can be obtained free of charge from The Cambridge Crystallographic Data Centre via www.ccdc.cam.ac.uk/data_request/cif); a) L. Palatinus, G. Chapuis, *J. Appl. Crystallogr.* **2007**, *40*, 786–790; b) G. M. Sheldrick, *Acta Crystallogr. Sect. A* **2008**, *64*, 112–122; c) O. V. Dolomanov, L. J. Bourhis, R. J. Gildea, J. A. K. Howard, H. Puschmann, *J. Appl. Crystallogr.* **2009**, *42*, 339–341.

[17] M. Mastalerz, I. M. Oppel, *Angew. Chem.* **2012**, *124*, 5345–5348; *Angew. Chem. Int. Ed.* **2012**, *51*, 5252–5255.

[18] M. J. Turner, J. J. McKinnon, D. Jayatilaka, M. A. Spackman, *CrystEngComm* **2011**, *13*, 1804–1813.

[19] S. Lowell, J. E. Shields, M. A. Thomas, M. Thommes, *Characterization of porous solids and powders: surface area, pore size and density*, Kluwer Academic Publishers, Dordrecht, **2004**, pp. 143–145.

[20] G. Férey, C. Mellot-Draznieks, C. Serre, F. Millange, J. Dutour, S. Surblé, I. Margiolaki, *Science* **2005**, *309*, 2040–2042.

[21] H. M. El-Kaderi, J. R. Hunt, J. L. Mendoza-Cortés, A. P. Côté, R. E. Taylor, M. O'Keefe, O. M. Yaghi, *Science* **2007**, *316*, 268–272.